frontiers in Marine Science

Evidence of Microplastic Size Impact on Mobility and Transport in the Marine Environment: A Review and Synthesis of Recent Research

Arefeh Shamskhany, Zhuoran Li, Preet Patel and Shooka Karimpour*

Department of Civil Engineering, Lassonde School of Engineering, York University, Toronto, ON, Canada

Marine Microplastics (MPs) exhibit a wide range of properties due to their variable origins and the weathering processes to which they are exposed. MP's versatile properties are connected to their dispersal, accumulation, and deposition in the marine environment. MP transport and dispersion are often explained by analogy with sediments. For natural sediments, one of the key features linked to transport and marine morphology is particle size. There is, however, no size classification defined for MP particles and MPs constitute all plastic particles sized smaller than the threshold of 5 mm. In this study, based on existing knowledge in hydrodynamics and natural sediment transport, the impact of MP size on turbulent entrainment, particle settling, and resuspension is described. Moreover, by analyzing several quantitative studies that have provided size distribution, size-selective accumulation of MPs in various regions of the marine environment is reported on. The preferential presence of MPs based on their size in different marine compartments is discussed based on the governing hydrodynamic parameters. Furthermore, the linkage between polymer properties and MP shape and size is explored. Despite the evident connection between hydrodynamic transport and MP size presented, classification of MP size presents challenges. MP size, shape, and density appear simultaneously in the definition of many hydrodynamic parameters described in this study. Unlike mineral sediments that possess a narrow range of density and shape, plastics are manufactured in a wide variety of densities and marine MPs are versatile in shape. Classification for MP size should incorporate particle variability in terms of polymer density and shape.

Keywords: marine microplastic pollution, particle size, hydrodynamics, entrainment and mixing, sediment transport

INTRODUCTION

Plastics are used for a wide spectrum of products and their production has increased drastically over the past decades. Due to improper or lack of end-of-life plastic management, plastic wastes appear globally from mountaintops (Napper et al., 2020) to seafloors (e.g., Van Cauwenberghe et al., 2013). Plastic emission to freshwater and marine environments occurs through various pathways such as stormwater runoffs, rivers, wastewater discharge, and wind. Once plastic debris reaches a body of

water, water acts as a transport vehicle and distributes and spreads the particles. Due to their slow decomposition processes, plastics can last in aquatic environments for centuries, if not millennia. In the past decade, concerns about Microplastics (MPs), plastic debris sized smaller than 5 mm, have emerged due to MP pollution impacts on the health of aquatic animals and humans. MPs can be ingested by various animals, ranging from microsized zooplankton (Cole et al., 2013) to whales (Fossi et al., 2012), and move up into the food chain. Furthermore, once ingested, toxins and microbes absorbed by MPs or accumulated on the surface can affect the host organism's health (Rochman et al., 2013; Lusher, 2015).

In marine and freshwater ecosystems, MPs have been reported in high concentrations both in the vicinity of their emission source, for instance, downstream of wastewater treatment plants (Murphy et al., 2016; Dalu et al., 2021), as well as in remote areas distant from the source (Huntington et al., 2020). Quantitative site-based studies in different water bodies have shown a varied assembly of MP properties in terms of their polymer, density, shape, and size (e.g., Morét-Ferguson et al., 2010; Naidoo et al., 2015). Many studies have identified the preferential presence of MPs based on their numerous properties in different compartments of aquatic systems (Thompson et al., 2004; Ryan, 2015; Baldwin et al., 2016; Cózar et al., 2017; Schwarz et al., 2019). Marine and freshwater MP particles are transported and dispersed by physical hydrodynamic processes. The importance and role of each process in MP mobility and deposition vary from site to site and are also dependent on MP properties (e.g., Zhang, 2017; Van Sebille et al., 2020).

One of the physical properties frequently associated with the distribution and mobility of MPs is density. Plastic density in freshwater and marine environments depends on the type of polymers and can be significantly affected by biofouling, that is the formation of biofilms on particles' surfaces (e.g., Long et al., 2015; Lagarde et al., 2016). Plastics with densities higher than the density of the ambient water are negatively buoyant and tend to sink, while plastics lighter than the ambient fluid are positively buoyant and tend to rise and float in a quiescent fluid (see **Figure 1**). For accumulation in surface water, for instance, some studies have found substantial quantities of polyethylene (PE) and polypropylene (PP) (e.g., Suaria et al., 2016), whereas others have identified polymers such as polystyrene (PS) to be abundantly present (e.g., Di and Wang, 2018). Review studies by Erni-Cassola et al. (2019) and Schwarz et al. (2019) have found PE and PP to be predominant in surface water, followed by PS. The overall data suggests that low-density polymers, PE and PP, both lighter than water, and PS, with densities only marginally different from that of water (**Table 1**), are predominant in surface water.

Similarly, MP shape is also linked to its mobility. MPs are either engineered as small-sized plastics, primary MPs, or they are the by-product of fragmentation of larger plastic debris, secondary MPs. While primary MPs are often in the form of spheres or pellets, secondary aquatic MPs exist in different shapes depending on their origin and exposure to fragmentation processes (Hidalgo-Ruz et al., 2012). Tanaka and Takada (2016), among others, presented shapes for MPs, from fragments and
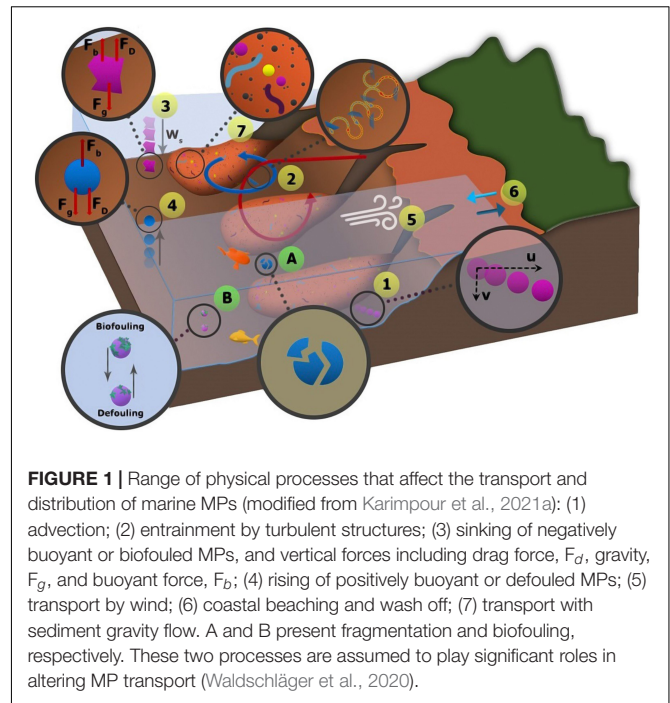

FIGURE 1 | Range of physical processes that affect the transport and distribution of marine MPs (modified from Karimpour et al., 2021a): (1) advection; (2) entrainment by turbulent structures; (3) sinking of negatively buoyant or biofouled MPs, and vertical forces including drag force, F_d, gravity, F_g, and buoyant force, F_b; (4) rising of positively buoyant or defouled MPs; (5) transport by wind; (6) coastal beaching and wash off; (7) transport with sediment gravity flow. A and B present fragmentation and biofouling, respectively. These two processes are assumed to play significant roles in altering MP transport (Waldschläger et al., 2020).

microbeads to sheets, films, and fibers. MP shape affects the particle's drag force, F_D, shown in **Figure 1**, and their rise and fall velocity (Kowalski et al., 2016; Khatmullina and Isachenko, 2017). The biofouling rate is also strongly linked to particle shape and the particles' exterior surface to volume ratio (Teuten et al., 2007; Kooi et al., 2017). Furthermore, sedimentary records have shown a higher presence of a specific MP shape, microfibers (Kane and Clare, 2019).

Another characteristic that can strongly impact MP dispersal is size. MPs are reported in a wide range of sizes across freshwater and marine compartments, varying from 10 μm to 5 mm (e.g., Reisser et al., 2015; Bergmann et al., 2017). Compared to natural sediments, the particle size of 5 mm, the upper size limit for MPs, is equivalent to the size of fine gravel, while the size of 10 μm is equivalent to that of silt. Among sediment properties, size classification is one of the most important sediment features affecting hydrodynamic transport and aquatic morphology (e.g., Heitmuller and Hudson, 2009; Yang and Shi, 2019). Despite its importance, a limited number of quantitative studies have sorted MPs based on size. In addition, in site-based quantitative studies that have provided size distributions, size classification and categories are inconsistent due to varying objectives, sampling locations and techniques, preparation, and analytical limitations. Filella (2015) has first highlighted the lack of attention to standardized size classification and its importance, using the sediment analogy. MP ingestion and ecological impacts are also tied to their size. Lehtiniemi et al. (2018) suggested that the size of MP fragments is a crucial factor, influencing the number of plastic particles ingested by small predators. In their study off the coast of South Africa for larger plastic debris, Ryan (2015) stressed the importance of plastic size in their long-distance transport. Furthermore, Kooi et al. (2017) noted the importance

TABLE 1 | Density of high-demand plastics (Harper and Petrie, 2003), seawater (25°C, salinity of 35 g/kg, 1 atm pressure), freshwater (4°C), and common range for mineral sediments.

Polymer type	Min (g/cm^3)	Max (g/cm^3)	Global plastic demand and distribution, 2019 (Plastics Europe, 2020)
Polyethylene (PE: LDPE, HDPE, LLDPE, MDPE)	0.88	0.97	29.8%
Polypropylene (PP)	0.90	0.92	19.4%
Polyvinyl chloride (PVC)	1.15	1.58	10.0%
Polyurethane (PUR)	0.01	1.26	7.9%
Polyethylene terephthalate (PET/PETE)	1.37	1.45	7.9%
Polystyrene (PS/EPS)	1.04	1.10	6.2%
Others	0.10	2.20	18.8%
Freshwater	1.000		–
Seawater	1.025		–
Mineral sand/silt/clay	2.50	2.80	–

The last column provides the global demand for each plastic polymer.

of size in MP biofouling and defouling. They have attributed size-dependent biofouling to the absence of finer MPs from the surface layers, reported by Cózar et al. (2014). Although the impact of MP size on some transport mechanisms has been discussed in several recent studies, a comprehensive understanding of this MP feature and its role in the mobility of MPs is still required.

In this study, some of the hydro-environmental factors that affect the transport of MPs are critically discussed. The impact of particle size and its linkage to these physical processes are explored in-depth. Furthermore, by consolidating the data on MP size distribution from different regions of the marine environment including sediments, the interconnections of size to transport process and accumulation are assessed. Evidence based on plastic composition and polymer types is also presented when reviewing the impact of polymer type and associated fragmentation rate on MP mobility. The objective is to provide a new narrative for MP size based on existing knowledge in sedimentology and to identify existing gaps in this area.

MICROPLASTIC SIZE IMPACT ON HYDRODYNAMIC PARAMETERS

Owing to the unique set of characteristics including their density, range, shape and morphology, MPs' behavior is different from that of natural sediments and other contaminants. Knowledge regarding the transport of natural sediments, however, can be utilized to formulate the unique hydrodynamic behavior of MP particles. In this section, the role of selected hydrodynamic processes in MP transport and their relation to particle size are discussed. **Figure 2** illustrates the role of particle size in MP response to the physical processes discussed in this section.

Effect of Size on Turbulent Mixing and Marine Microplastic Entrainment

In turbulent flow, the particle entrainment process is an interplay of turbulence features, gravitational effects, and particle morphology. This interaction between the turbulent flow and gravitational effects of particles appears in different scales of the flow, from larger integral-scale eddies to small dissipative

Kolmogorov's scale. The energy-containing eddies are presented by the integral scale, while the viscous range is presented by the Kolmogorov's scale. In formulating this interaction, parameters associated with turbulence length and time scales must be accounted for. The larger scale of turbulence is presented by integral length, l, and turnover time scale, τ_l. The small Kolmogorov's time, τ_υ, and length scale, η, are defined as (e.g., Good et al., 2014):

$$\tau_\upsilon = \left(\frac{\upsilon}{\varepsilon}\right)^{1/2}; \ \eta = \left(\frac{\upsilon^3}{\varepsilon}\right)^{1/4} \quad (1)$$
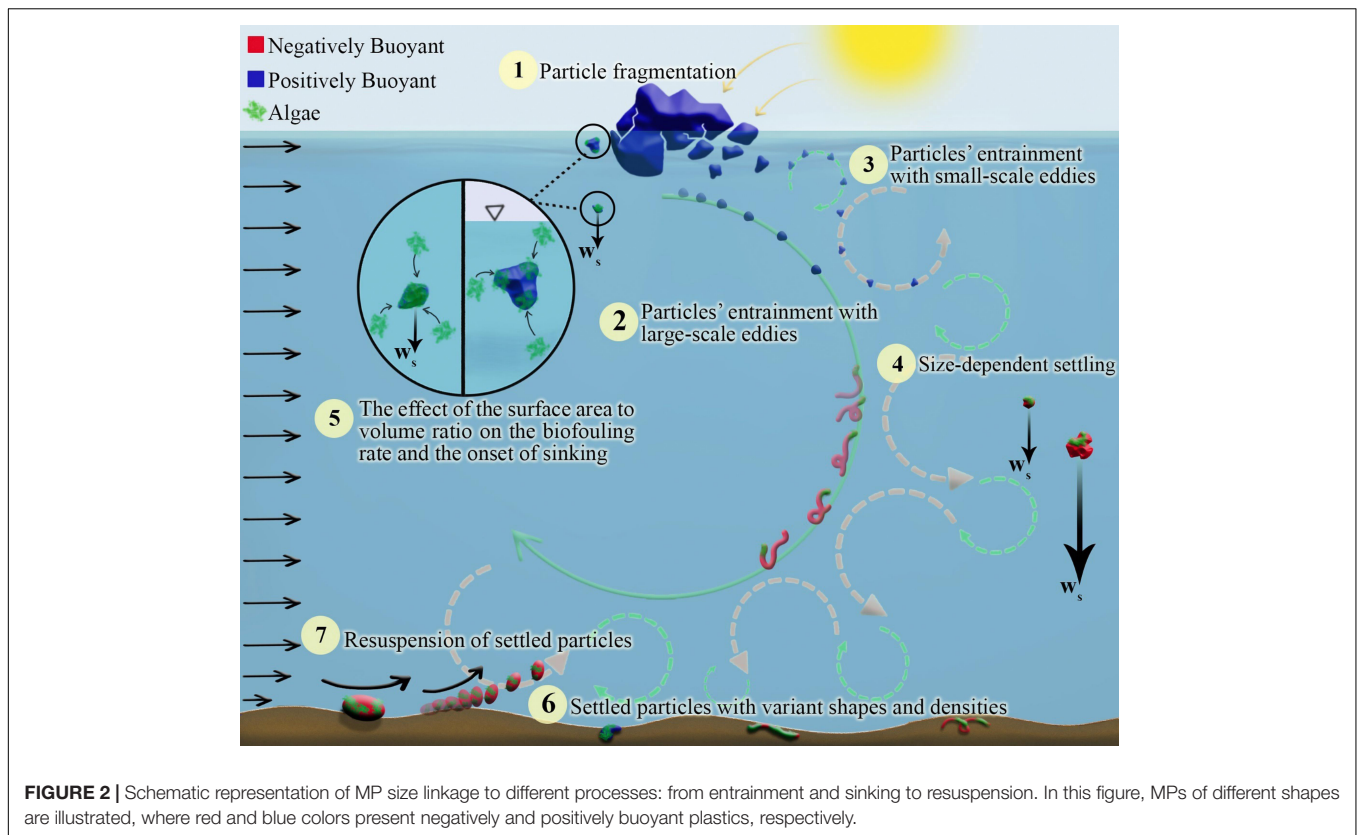
where υ is the kinematic viscosity of the fluid and ε is the dissipation rate per unit mass. Particle engagement also depends on particle size and density, as well as the density of the ambient fluid (Dey et al., 2019). These factors are reflected in particle relaxation time, τ_p:

$$\tau_p = \frac{d^2 \left(\rho_p - \rho_w\right)}{18\mu} \quad (2)$$

where d is the particle diameter, ρ_p is the particle density, ρ_w the density of the ambient water, and μ is the dynamic viscosity of fluid. The particle relaxation time is sometimes defined by the absolute density (e.g., Wang and Maxey, 1993); however, the more general equation considers the density difference between the particle and the ambient fluid, as demonstrated in Eq. (2) (Wang et al., 2018). Two dimensionless parameters, based on turbulent time scales and particle relaxation time, can be defined to describe the relative significance of natural vertical movements of particles due to gravity and buoyancy, compared to turbulent-induced particle entrainment. The effects of small-scale turbulence on particle motion are ascertained by the Stokes number as defined by Kolmogorov's time scale:

$$St_\upsilon = \frac{\tau_p}{\tau_\upsilon} \quad (3)$$

The integral time and length scale are dependent on the magnitude of the geometry of the problem, as well as the initial instability conditions (e.g., Karimpour and Chu, 2019;

FIGURE 2 | Schematic representation of MP size linkage to different processes: from entrainment and sinking to resuspension. In this figure, MPs of different shapes are illustrated, where red and blue colors present negatively and positively buoyant plastics, respectively.

Karimpour et al., 2021b). The effect of integral scale eddies on entrainment is formulated using the integral time scale:
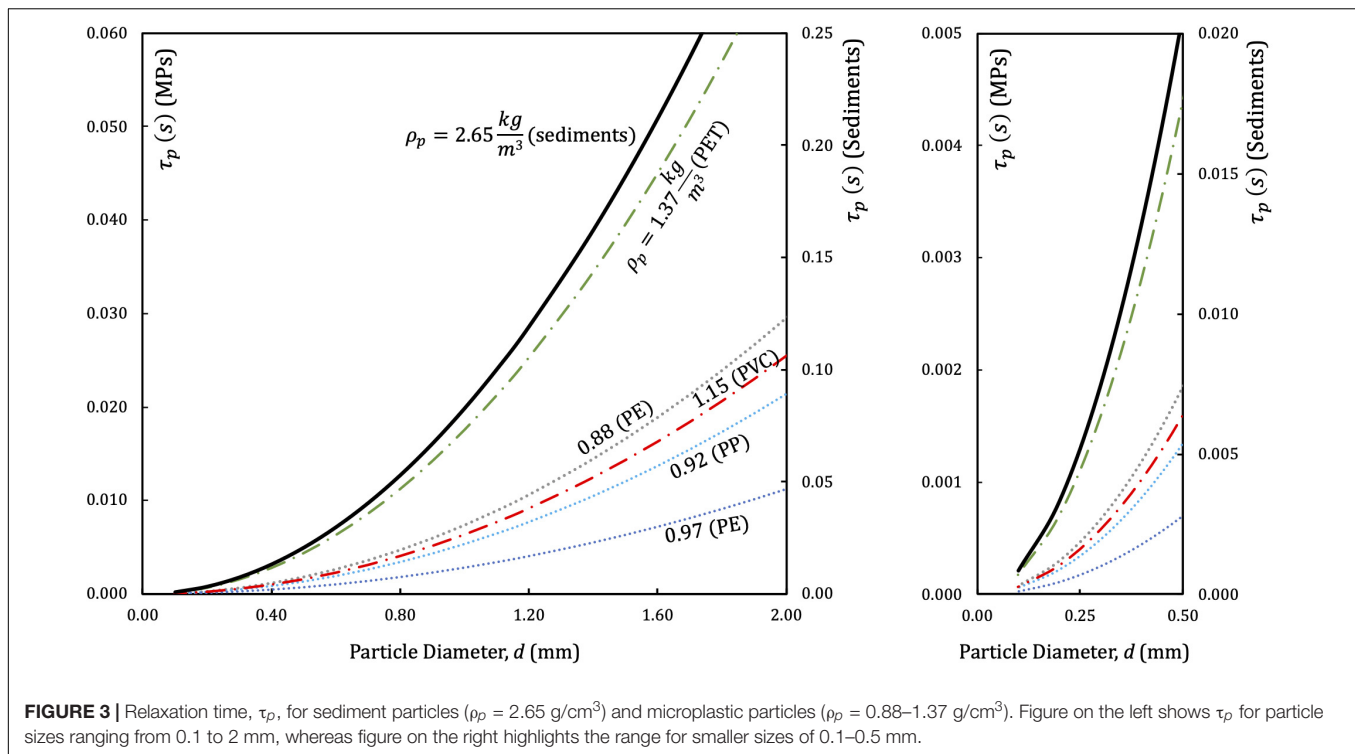
$$St_l = \frac{\tau_p}{\tau_l} \qquad (4)$$

Large Stokes numbers associate with higher particle relaxation time or smaller turbulence time scales. In such conditions, particle engagement with the ambient structure lags, and particles move following their natural sinking or rising behavior. For suspended sediments, large Stokes numbers lead to sinking and deposition to bed. On the contrary, for small Stokes numbers, particles are entrained in the flow and when the Stokes number is very low, particle behavior will be similar to that of a passive scalar. The relevance of these two dimensionless Stokes numbers depends on the particle's size compared to integral and Kolmogorov's length scales (e.g., Gorokhovski and Zamansky, 2018).

As can be seen in Eq. (2), particle relaxation time, τ_p, is a function of the particle size, d, as well as the particle's marginal density from that of ambient water, $(\rho_p - \rho_w)$. Sediment particle density, composed of minerals, is typically between 2.50 to 2.80 g/cm^3. Plastics, on the other hand, possess a wide range of densities: density of foamed PS is a fraction of the density of water, PS can be marginally heavier or lighter than water, whereas PVC can be up to 60% heavier than seawater and freshwater. About 50% of plastics have densities within the 20% margin of seawater and freshwater densities (**Table 1**). The most common polymer types, PE and PP, are marginally lighter than seawater.

Figure 3 is the plot of relaxation time for sediment particles with density of $\rho_p = 2.65$ g/cm^3, positively buoyant plastics with densities between 0.88 and 0.97 g/cm^3, and negatively buoyant plastics with densities of 1.15 and 1.37 g/cm^3. These densities are selected as they represent the minimum and maximum ranges of some of the most common polymer types listed in **Table 1**. Particles with smaller marginal density compared to that of seawater, e.g., 0.97 g/cm^3, correspondingly have a very low overall relaxation time.

A sand particle with a diameter of 0.2 mm, has a relaxation time of about $\tau_p = 0.0036$ s. This relaxation time is attributed to the small particle diameter and marginal density, $(\rho_p - \rho_w)$. Particles smaller than fine sands (including silt and clay) are often entrained with the ambient flow and are transported to distant areas where samples from deep sediments often include silt, clay, and fine sands (e.g., Cunningham et al., 2020). However, MPs have a lower marginal density compared to natural sediments. Therefore, for a turbulent flow with an integral time scale of τ_l and Kolmogorov's time scale of τ_ν, MP particles identical to sediments in terms of size and shape exhibit lower Stokes numbers. Due to the lower marginal density of MPs, larger MP particles may entrain in various scales of the turbulent flow. For instance, for a density of 0.88 g/cm^3 and 1.37 g/cm^3, MPs with diameters of 0.7 and 0.4 mm, respectively, exhibit the same relaxation time as sand particles with a diameter of 0.2 mm. For a MP particle, made of heavy PE with a density of 0.97 g/cm^3, particles with a diameter of 1.15 mm exhibit a similar range of relaxation time as fine sand particles. Due to their smaller

FIGURE 3 | Relaxation time, τ_p, for sediment particles (ρ_p = 2.65 g/cm^3) and microplastic particles (ρ_p = 0.88–1.37 g/cm^3). Figure on the left shows τ_p for particle sizes ranging from 0.1 to 2 mm, whereas figure on the right highlights the range for smaller sizes of 0.1–0.5 mm.

marginal density in turbulent flow, MP particles deviate from their natural sinking or rising behaviors as defined by their density. A combination of MP's marginal density and size will govern the process. As demonstrated in **Figure 2**, small size MP particles with small marginal density can be entrained and transported to areas distant from MP emission sources.

Rising and Settling Velocities of Microplastics

MP particles can either be positively or negatively buoyant, leading to the rising or settling of these contaminants in a motionless water column (**Figure 1**). The rising and settling velocities of MP particles are often assumed to be calculated similarly to those of natural sediments with similar characteristics (e.g., Waldschläger and Schüttrumpf, 2019). However, MP particles have shapes that exhibit complex sinking or rising behaviors (Tanaka and Takada, 2016). In motionless fluid, assuming that vertical forces are limited to gravity, buoyancy, and drag, the steady state particle velocity, w_p, can be estimated based on the following equation:

$$\frac{1}{2} C_D \rho_w A_p w_p^2 \; = \; |\rho_p - \rho_w| gV \tag{5}$$

where C_D is the drag coefficient and depends on particle shape and flow regime (e.g., Clift et al., 1978; Chubarenko et al., 2018), A_p is the particle projected area resisting the relative fluid motion, and V is the volume of the particle. Re-arranging Eq. (5) yields:

$$w_p = \sqrt{\frac{2g}{C_D} \frac{|\rho_p - \rho_w|}{\rho_w} \frac{V}{A_p}} \tag{6}$$

In Eq. (6), the volume to projected area ratio, V/A_p, is affected by particle shape which plays a key role in the settling pattern of MPs as it influences the drag coefficient as well as the volume to projected area ratio. MP shape can further affect the sinking or rising behavior of particles in favorable biofouling conditions (see section "Biofouling"). The volume to projected area ratio additionally signifies the role of particle size on settling and rising velocities. The particle size also affects the flow regime that is surrounding the MP particle by impacting the particle's Reynolds number:

$$\mathrm{Re}_p = \frac{w_p d}{\upsilon} \tag{7}$$

For laminar particle Reynolds number, the drag coefficient is larger for smaller particles. Along with a smaller volume to projected area ratio, V/A_p, this leads to a smaller steady state rising or settling velocity for finer particles. For MPs, Kooi et al. (2017) have shown the sinking velocity variability with size. Similar to Eq. (2) for particle relaxation time, Eq. (6) for settling and rising velocity is derived from the particle's force balance, therefore, marginal density, ($\rho_p - \rho_w$), also appears in this equation. Due to a smaller marginal density in comparison to mineral sediment particles, MPs exhibit smaller settling velocities. The settling velocity of an MP particle with a density of 1.30 g/cm^3 is about 2.3 times slower than the settling velocity of a similarly sized and shaped sediment particle. The ratio for an MP particle of a density of 1.10 g/cm^3 is about 4.0. This leads to longer exposure of small MP particles to in-depth currents and mixing induced by waves, roller, and other wind-induced structures, as well as structures such as thermohaline circulations.

Such entrainment and mixing of MP particles, as evidenced by the Stokes number, results in inhibited sinking and rising.

Biofouling

Biofouling is an important mechanism that impacts the buoyancy of MPs in aquatic systems. The growth and accumulation of microbes, algae, and invertebrates alter the density of MPs, affecting their buoyancy and sinking or rising patterns (Ye and Andrady, 1991; Long et al., 2015). Some of the environmental parameters that affect biofilm formation, growth rate, and composition are depth profiles of light extinction, salinity, density, and viscosity (Kooi et al., 2017). Due to the variability of these environmental factors, the biofouling effect on MP vertical transport is reported to vary in different marine regions and seasons (e.g., Artham et al., 2009; Kaiser et al., 2017). Biofouling formation also depends on polymer composition, surface energy, and the particle's surface roughness (Artham et al., 2009; Andrady, 2011).

For naturally buoyant particles, biofouling results in an increase in apparent density and ultimate sinking. Biofouling also affects the settling behavior of negatively buoyant and naturally sinking particles (Rummel et al., 2017). The change in apparent density of biofouled MPs is directly related to the exterior surface area to volume ratio. This exterior surface area to volume ratio is affected by MP shape (e.g., Ballent et al., 2016; Fazey and Ryan, 2016) and size (Kooi et al., 2017). Based on the exterior surface to volume ratio analysis, Chubarenko et al. (2016) suggested that, for MP shapes of smaller characteristic length in similar environmental conditions, the impact of biofouling progression on density appears faster. Therefore, among different MP shape categories, those with a larger exterior surface area to volume ratio, such as fibers and filaments, will sink faster when exposed to biofouling in contrast to fragments and beads which are slower to respond to biofouling. Kaiser et al. (2017) suggested, however, that even in similar environments, the biofilm composition may be dependent on MP shape. Especially in microfibers, small exterior surface areas and characteristic length may prevent the attachment of some macro-foulants.

For MP particles of similar shapes, when particles are small, due to their large exterior surface area to volume ratio, the buoyancy changes immediately after the particle is exposed to biofouling. On the other hand, for larger particles, the impact of biofouling on particles' buoyancy only emerges after longer exposure, as illustrated in **Figure 2**. Kooi et al. (2017) evaluated settling onset time with different particle radii and densities. For spherical particles of different buoyant polymer types, the sinking onset was estimated at about 26 days for those with a radius of 1–10 mm, while the onset for smaller particles was estimated to occur more rapidly.

Moreover, the impact of biofouling on MP sinking behavior is complex and not solely due to the change in the particle's density. The accumulation of biofilm may alter the overall shape of the particles and affect their roughness. Furthermore, biofilm aggregates can be permeable, affecting the vertical transport patterns (Xiao et al., 2012; Long et al., 2015). Change of buoyancy due to biofouling is evidently affected by the plastic size, where smaller buoyant MPs change buoyancy faster. However, further

studies will be required to examine the sinking behaviors of various sized and shaped MPs with different fouling conditions.

Critical Velocity for Resuspension

Negatively buoyant particles that have settled experience shear stress caused by flow velocity. The shear stress exerted on settled particles eventually reaches a value that will force the particles to resuspend, get entrained with the ambient flow, and be transported. A major advancement in sediment resuspension threshold determination was provided by the Shields diagram (Shields, 1936). The threshold developed by Shields (1936) is based on dimensional analysis where:

$$\text{Threshhold} = f\left(\upsilon, d_s, \tau_o, \rho_s, \rho_w, g\right) \tag{8}$$

which yields:

$$\frac{\tau_o}{(\rho_s - \rho_w)gd_s} = f\left(\frac{u_* d_s}{\upsilon}\right) = f\left(\frac{d_s}{\delta}\right) \tag{9}$$

where δ is the thickness of the viscous sublayer, d_s is the sediment size, ρ_s is sediment particle density, and τ_o is the shear stress. The ratio of particle to viscous sub-layer thickness on the right-hand side of Eq. (9), d_s/δ, is defined as the boundary layer Reynolds number, Re_*. Based on the shear stress, τ_o, shear velocity is defined as $u_* = \sqrt{\tau_o/\rho_w}$, which is a measure of the shear stress in the flow. The dimensionless variable on the left-hand-side denotes the ratio of forces acting on a particle affecting its motion and is recognized as Shields number, θ. The Shields diagram identifies the motion threshold based on the Shields number, θ, as a function of the boundary layer Reynolds number, Re_*. The Shields diagram and its variants are discussed in Miller et al. (1977). Similar to sediment particles, MPs that have settled in sediments are prone to resuspension. Chubarenko et al. (2018) have plotted experiments by Ballent et al. (2012) for MP pellets on the Shields diagram and identified the discrepancies in behavior observed between Shields material and MPs. Kane et al. (2020) have used the Shields number to assess the mobility of sedimentary MPs. Re-writing dimensional analysis and incorporating MP particle density, ρ_p, and size, d_p, the MP resuspension threshold becomes:

$$\text{Threshhold for MP Particles} = g\left(\upsilon, d_s, \tau_o, \rho_s, \rho_w, g, d_p, \rho_p\right) \tag{10}$$

which yields:

$$\frac{\tau_o}{(\rho_p - \rho_w)gd_p} = g\left(\frac{u_* d_s}{\upsilon}, \frac{d_s}{d_p}\right) \tag{11}$$

In Eq. (11), the Shields number, θ, is defined based on MP density, ρ_p, and size, d_p, as this dimensionless number denotes the forces on a MP particle. On the other hand, the boundary layer Reynolds number, Re_*, is governed by bed roughness size, for sediments denoted by d_s, and δ that is the thickness of the viscous sublayer. The impact of sediment to settled MP particle size ratio, d_s/d_p, on boundary layer development is not clear. However, in a few studies on sedimentary MPs, authors have reported sediment aggregate size and alluded to its potential impact on boundary

layer development and resuspension thresholds (Cunningham et al., 2020; Kane et al., 2020).

The impact of MP size on resuspension is clearly demonstrated in Eq. (11). MPs with a smaller characterized dimension, d_p, possess a higher Shields number, and are of greater probability to exceed the threshold of motion. The fine settled particles are more likely to resuspend in a weak flow field and surrender to long-distance transport. The particle's marginal density, $(\rho_p - \rho_w)$, also appears in the definition of this hydrodynamic parameter. With a marginal density difference between the ambient water and MP, smaller shear stresses and shear velocities lead to the resuspension of MPs.

EVIDENCE OF SIZE-SELECTIVE DISTRIBUTION AND TRANSPORT

For this section, literature on marine MP presence and detection is systematically reviewed, focusing on studies that have investigated size and density in various marine compartments. Among more than 200 reviewed studies, although many have reported the size range, only 15 provided size distribution for MP particles. These studies are summarized in **Table 2** and categorized on the basis of the region of the study and vicinity to nearshore for both sediments and surface water. The depth of the sampling is governed by the sampling method. In studies listed for surface water, a variety of sampling techniques, including bulk and volume-reduced sampling methods, were used. In volume-reduced methods employing manta and neuston nets listed in **Table 2**, the depth of the sampling did not exceed 75 cm from the free surface. While for the bulk sampling employed by Enders et al. (2015), the inlet of the pump was submerged to a depth of 3.0 m below the free surface. For studies in sediments, the depth of sampling was measured from the bed and was limited to 65 cm.

The reported abundance, concentration, and polymer type depend on source vicinity, discharge routes, and locally used plastics. The size distribution, however, is an indication of flow hydrodynamics dominating the MP spread and dispersal. Despite the provision of the size range in many reviewed studies, the size distribution is not widely available. In studies that have provided size distribution, there is no standardized size classification as observed by Filella (2015). Furthermore, the lower and upper size limits are bounded by sampling and analytical methods, as well as the objective of the study (see **Table 2** for size range). The lack of a unified and standardized approach amongst different studies has limited the analysis presented in this paper. However, the size distribution in these studies provides insight into the frequency and concentration of various size categories and qualitative descriptions of size distribution profiles.

Impact of Marine Microplastic Size on Surface Water Presence

Waves and currents in coastal regions are the most important factors in the transport, erosion, and deposition of sediments (Inman and Masters, 1991). In nearshore areas, the effect of breaking waves along with the presence of longitudinal currents generated by waves creates a size-selective distribution of sediments. This leads to a heterogeneous sediment distribution, with coarse material remaining on the beach and fine material being washed away. Inman and Bagnold (1963) were among the first to examine nearshore sand distribution based on their size. Finn et al. (2016) analyzed the motion of coarse and fine sand particles under passing surface waves, and found strong spatiotemporal particle size sorting patterns, where vertical size sorting of grains in suspension has been reported. Correspondingly, for microplastics, transport and entrainment induced by coastal sub-surface currents and vortices are size-dependent.

Ryan (2015) has reported the size distribution for plastic debris in nearshore and offshore sites for plastic pieces sized smaller than 60 cm. In the coastal areas, the results indicate that about 60% of plastic pieces were sized smaller than 5 cm. While in offshore regions, about 65% of plastics were sized between 5 to 30 cm. This shows a preferential abundance of larger floating plastic pieces offshore in surface water.

Figure 4 reports the size characteristics for studies in **Table 2** that provided size distribution for surface water in nearshore and offshore regions. In this figure a few features are extracted from the size distribution reported in the original studies: peak size distribution and D_{50}, or vicinity thereof. The peak size boxes in **Figure 4** have variable sizes as the bin sizes vary in different studies. D_{50} is the particle diameter at 50% in the cumulative distribution, demonstrated by a horizontal line for each study. Chae et al. (2015), Qu et al. (2018), and Sagawa et al. (2018) are among the studies that investigated the size distribution of microplastics in coastal areas. The peak size bins in all three studies lie between 100 and 750 μm, whereas D_{50} is approximately smaller than 1,200 μm as shown in **Figure 4A**.

Offshore studies, shown in **Figure 4B**, reported peak frequency or concentration at larger size categories. The peak size bin varies from Reisser et al. (2015), who have reported a peak size of 500–1,000 μm, to Morét-Ferguson et al. (2010) with a peak of 3,000–4,000 μm. Morét-Ferguson et al. (2010) have also used larger bin sizes to provide size distribution. The peak of the distribution, however, lies at a larger size. Furthermore, the vicinity of D_{50} is also identified at a larger size range. Enders et al. (2015) have looked at individual MP particle and fiber size. The mean size reported for particles with shapes other than fibers was notably smaller for both nearshore and offshore regions compared to other studies, as demonstrated in **Figure 4C**. They, however, reported mean size values from nearshore samples that were smaller compared to samples extracted from offshore, open ocean, and subtropical gyres.

For low-density buoyant MPs, with apparent density lower than that of seawater, particle size affects the relaxation time. Smaller MPs have smaller particle relaxation times. Therefore, as buoyant plastics and MPs reach coastal areas, small-sized particles are more likely to separate from the surface layer and get entrained with wave-, wind-, or thermal-induced currents and subsequently get advected and transported offshore. Additionally, small MPs have a larger exterior surface area to volume ratio and therefore, when exposed to biofouling, their onset of sinking is shorter. Due to the combined influence
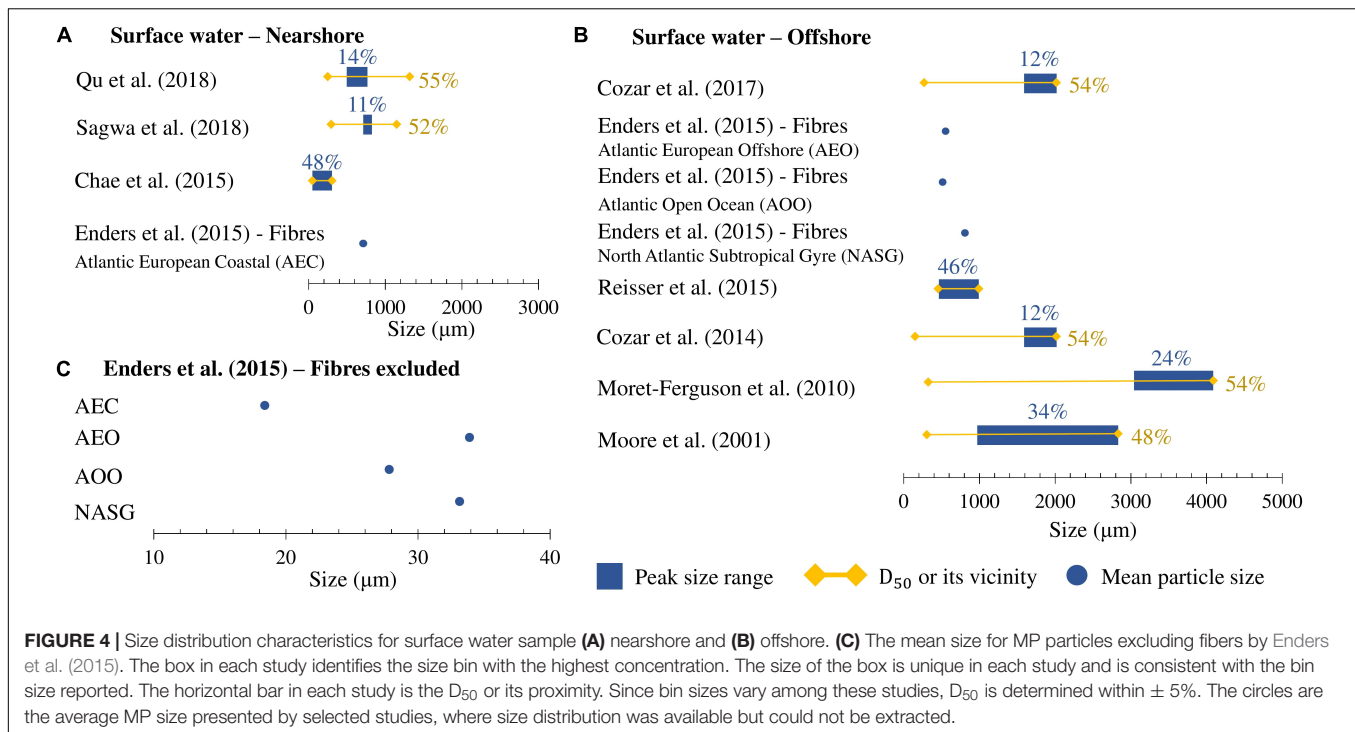
TABLE 2 | Studies that have identified the size distribution of MPs in nearshore (NS) and offshore (OS) water and offshore sediments.

	Source	Location	Sampling depth (cm)	Sampling technique	Size range (μm)	Dominant shape
Surface water–NS	Qu et al. (2018)	Coastal waters of China	not available	Volumetric steel samplers	[20, 5,000]	Fibers
	Sagawa et al. (2018)	Hiroshima Bay, Japan	0.00–75.00[A]	Neuston net; 75 × 75 × 300 cm^3	(355, 5,000)	–
	Chae et al. (2015)	Korean West Coast	0.00–0.04	Stainless steel sieve; 20 cm diameter	[50, 1,000]	–
	Enders et al. (2015)	Atlantic European Coastal	0.00–300.00	Volumetric sampling using pump	[10, 10,000]	Other than fibers
Surface water–OS	Cózar et al. (2017)	Mediterranean Sea		Manta net; 86 cm width	[320, 860]	
		Arctic Ocean	0.00–15.00			Fragments
		Subtropical Gyres				
	Enders et al. (2015)	North Atlantic Subtropical Gyre	0.00–300.00	Volumetric sampling using pump	[10, 10,000]	Other than fibers
		Atlantic Open Ocean				–
		Atlantic European offshore				–
	Reisser et al. (2015)	North Atlantic sub-tropical gyre	0.00–50.00	Filter net	[500, 5,500)	Fragments
	Cózar et al. (2014)	Malaspina Circumnavigation	0.00−-50.00[A]	Neuston net; 50 × 100 cm^2	[200, 10,000]	Fragments and Sheets
	Morét-Ferguson et al. (2010)	Atlantic Ocean	0.00–25.00	Neuston net; 50 × 100 cm^2	[335, 15,000)	Fragments
	Moore et al. (2001)	North Pacific Central Gyre	0.00–15.00[A]	Manta trawl; 15 × 90 × 350 cm^3	[355, 4,760]	Fragments
Sediment–OS	Courtene-Jones et al. (2020)	Rockall Trough, North Atlantic Ocean	0.00–60.00	Sediment core samples; 60 cm height and 10 cm diameter	[52, 6,500)	Fibers
	Zhang et al. (2020)	Western Pacific Ocean	0.00–5.00	Stainless-steel box corer	[100, 5,000]	Fibers
	Cordova and Wahyudi (2016)	Eastern Indian Ocean	0.00–60.00[B]	Main samples: box corer; 60 × 40 × 50 cm^3; Sub-samples: stainless steel shovel	(20, 500)	Granules
Arctic Sediment–OS	Tekman et al. (2020)	Arctic Ocean	0.00–5.00	A video-guided multiple corer with eight cores of 100 mm diameter	[11, 100]	Fibers
	Mu et al. (2019)	Arctic Ocean	0.00–65.00[B]	Stainless-steel box corer; 50 × 50 × 65 cm^3	[100, 2,000]	Fibers
	Bergmann et al. (2017)	Arctic Ocean	0.00–5.00	A video-guided multiple corer with eight cores of 100 mm diameter	[11, 500)	–

In surface water sampling, depth indicates the depth from the free surface, while in sediments, depth is measured from the bed. Size limitation indicates the minimum threshold dictated by sampling and/or characterization method. Square brackets in size range indicate that the size range is limited to the endpoint, whereas round parentheses mean size range contains values beyond the endpoint.
[A]*Water depth was not explicitly provided. Therefore, the maximum net mouth dimension is assumed as the depth.*
[B]*Sediment depth was not available. Therefore, the maximum core dimension is assumed as the depth.*

FIGURE 4 | Size distribution characteristics for surface water sample **(A)** nearshore and **(B)** offshore. **(C)** The mean size for MP particles excluding fibers by Enders et al. (2015). The box in each study identifies the size bin with the highest concentration. The size of the box is unique in each study and is consistent with the bin size reported. The horizontal bar in each study is the D_{50} or its proximity. Since bin sizes vary among these studies, D_{50} is determined within $\pm$ 5%. The circles are the average MP size presented by selected studies, where size distribution was available but could not be extracted.

of biofouling effect and higher potential for entrainment, they appear less abundant in offshore surface water samples.

Similarly, for fine negatively buoyant MPs, biofouled or pristine, entrainment with in-depth vortices and their offshore transport can be induced by weaker currents. This is further reinforced as smaller negatively buoyant particles sink gradually. Therefore, the presence of small-sized high-density MPs, both biofouled and pristine, in the water column is prolonged. This increases the likelihood of entrainment over time. While, for larger sinking MPs, only strong currents can entrain the particles and lead to offshore transport. Furthermore, the resuspension and mobility of settled MPs are also size dependant. Smaller sized MPs that have settled have a higher Shields number, θ, which leads to a lower resuspension threshold, and a higher likelihood of resuspension.

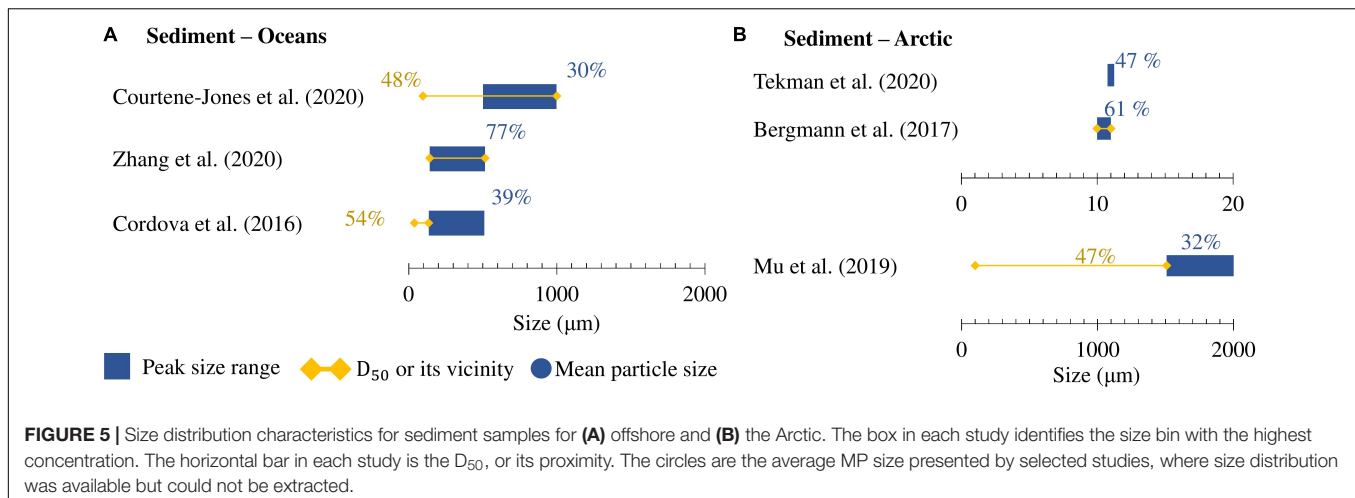## Deep-Sea Marine Microplastic Presence

Once sediments are transported by fluvial means into marine environments, larger sediments, such as sand, settle in shallower marine environments in nearshore areas. Smaller sediments, such as silt and clay, remain entrained in the currents and are transported offshore. These particles are carried to regions with lower velocity currents and, with a very slow rate, are deposited to the bed. Another main mechanism leading to the bed deposition of sediments is turbidity currents. Turbidity currents originate over continental shelves, where high-density sediment-laden flow plunges down to the seabed. These currents are the primary processes for carrying fine sand to deep-sea sediments. Similarly, MP debris accumulates in seafloor sediments either directly by sinking through the water column, or *via* currents and sediments transported from the fluvial regions

(Clark et al., 2016; Kane and Clare, 2019). Some studies suggest that deep-sea sediments can be the sink for lost MPs (e.g., Anderson et al., 2016; Chiba et al., 2018). However, Barrett et al. (2020) have shown the contrary, where the sedimentary deep-sea MPs account for only a small portion of lost MPs. Nevertheless, our analysis of the existing studies on size distribution in nearshore and offshore areas on surface water shows that smaller MPs are missing from the water surface. This corroborates findings by Cózar et al. (2014) that have shown a size-selective absence of MPs from the ocean surface.

Figure 5A shows the peak bin size with the highest concentration and D_{50}, or its proximity, for deep-sea sediments. D_{50} in all cases falls below 1,000 μm, and this value never exceeds the peak bin size. This signifies the abundance of narrow particle size distribution that is limited to very fine MPs in deep-sea sediments. For nearshore surface water samples, although the peak size bin was also reported to be small, D_{50} extended beyond this size showing a wider spread of size distribution. This is attributed to the impact of size in hydrodynamic processes outlined in section "Microplastic Size Impact on Hydrodynamic Parameters." Intrusion of fine MPs in deep-sea sediments can partly explain the absence of these MPs from the water surface in offshore regions.

Remote Areas and Size Distribution

In recent years, the prevalence of MPs in remote Arctic and Antarctic regions has drawn the attention of researchers around the world. MP particles have been found in Arctic and Antarctic surface water (Cózar et al., 2017; Huntington et al., 2020; Tekman et al., 2020) as well as in deep-sea sediment samples (Bergmann et al., 2017; Mu et al., 2019; Huntington et al., 2020;

FIGURE 5 | Size distribution characteristics for sediment samples for **(A)** offshore and **(B)** the Arctic. The box in each study identifies the size bin with the highest concentration. The horizontal bar in each study is the D$_{50}$, or its proximity. The circles are the average MP size presented by selected studies, where size distribution was available but could not be extracted.

Tekman et al., 2020; Adams et al., 2021). The high abundance reported had no correlation with upstream population and was associated with long-distance transport from remote sources (Huntington et al., 2020). Thermohaline currents are among the important processes in the transport of deep fine sediments (Rebesco et al., 2014), and Cózar et al. (2017) attributed the prevalence of MPs in Arctic remote areas to these global currents. The shallow thermohaline currents can redistribute floating plastics from different latitudes (Cózar et al., 2017). On the other hand, deep thermohaline currents will interact with deep-sea sediments and sediment currents, and transport settled, settling, and neutrally buoyant MP pieces (Kane and Clare, 2019).

A few studies have provided the size distribution of MPs in the sediments extracted from Arctic regions (**Figure 5**). All these studies have noted the abundance of fine MPs in sediment samples. In fact, Bergmann et al. (2017) have reported that about 80% of MP particles were sized smaller than 25 μm. The mobility of MP particles induced by the thermohaline currents is dependent on their size. The shear velocity imposed by deep thermohaline currents can lead to resuspension of fine sediments, as well as fine MPs. The turbulent structures induced by this velocity gradient in a thermohaline current (Radko, 2019) can lead to the entrainment and long-distance transport of sediment and MP particles, depending on their size and relaxation time.

POLYMER TYPE AND RELATION TO PARTICLE SIZE AND SHAPE

Plastics are made of different polymers with a wide variety of properties. Plastic density has been highlighted as one of the important properties affecting transport and distribution. Density evidently impacts aquatic MP distribution as it affects the buoyancy of the particle in quiescent fluid. In recent years, Erni-Cassola et al. (2019) and Schwarz et al. (2019) have looked at plastic distribution in different freshwater and marine regions. Schwarz et al. (2019) have consolidated literature on marine sediments, while Erni-Cassola et al. (2019) have gathered

evidence on polymer type accumulation in intertidal, subtidal, and deep-sea sediments separately. Both studies have discussed the selectiveness of MP distribution based on density.

Plastics, however, possess other properties that affect their distribution; among these properties are brittleness and flexibility. **Table 3** presents two material properties: Young's Modulus of elasticity, in MPa, and Elongation, in percentage. Young's Modulus is a measure of the ability of a material, plastics in this case, to withstand changes in length when it undergoes tension or compression. Elongation, on the other hand, is a measure of deformation before a material breaks if subjected to a tensile load. Plastic polymers such as HDPE, LDPE, PUR, and PP, have high elongation and can be categorized as ductile, while hard plastics such as PVC, PS, and PET have relatively lower elongation. All three polymers also have high Young's Modulus of elasticity and are more brittle than other plastics listed. This is consistent with the study by Efimova et al. (2018) that examined the fragmentation rate for PS, PS foam, LDPE, and PP. They reported that PS, listed with the lowest elongation in **Table 3**, has the highest fragmentation rate and after 15–18 days of mixing with sediment and water it reached about 80% fragmentation in the form of MPs, in terms of its original mass. Whereas, for PP, a ductile plastic polymer, only 0.07% of the original mass was fragmented into MPs after about 24 days of mixing. Due to their low brittleness, HDPE, LDP, PUR, and PP are resistant to fragmentation. Whereas fast fragmentation to smaller plastics and eventually to smaller-sized MPs is anticipated for PVC, PS, and PET.

As described in section "Microplastic Size Impact on Hydrodynamic Parameters," long-distance transport is size-selective. Given that PVC, PS, and PET are fragmented rapidly, under favorable conditions, they will most likely be entrained and transported farther. The meta-analysis by Erni-Cassola et al. (2019), clearly demonstrated this polymer selectiveness, established by a combination of fast fragmentation, density, and impact of size on transport. In their analysis for subtidal and intertidal sediments, they reported a concentration of between 25 and 40% for polyester, polyamide, and acrylic. Whereas, in deep-sea marine sediments their compilation yielded a higher

TABLE 3 | Young's modulus of elasticity and elongation for selected polymer types (Harper and Petrie, 2003).

Polymer type	Young's modulus (MPa)	Elongation (%)
Polyethylene, HDPE	1,069–1,089	10–1,200
Polyethylene, LDPE	172–282	100–650
Polypropylene (PP)	1,138–1,551	100–600
Polyvinyl chloride (PVC), hard	2,413–4,137	40–80
Polyurethane (PUR)	0.17–34.47	250–800
Polyethylene terephthalate (PET/PETE)	2,758–4,137	30–300
Polystyrene (PS/EPS)	2,275–3,275	1.2–2.5
Polyamide (PA6)	2,000	65–150
Polyamide (PA66)	1,586–3,447	150–300

concentration of roughly 75% for polyester, polyamide, and acrylic. The demand for polyester, made of PET, is about 8% and demand for polyamide is 2%. If the density is considered as the sole plastic property governing the distribution, all land-based debris pieces composed of PET, polyamide, and acrylic should settle nearshore as these polymers have densities higher than those of both seawater and freshwater. Due to their high fragmentation rate and smaller size, particles made of these polymers can be transported offshore and settle in areas with slow ambient velocities. The high concentration of polyester, polyamide, and acrylic in deep-sea sediment is due to the combination of polymer properties, including their brittleness, measured by elongation and density, as well as particle's shape. The presence of small-sized MPs, based on the evidence presented in this paper, along with the abundance of polyester, polyamide, and acrylic in deep-sea sediments conform with observations reported for MP shape in this compartment. All the studies listed in **Table 2** for deep-sea sediments have reported MP shape categories. Courtene-Jones et al. (2020) and Zhang et al. (2020) have distinctly reported fibers as the dominant shape. Microfibers are also found in higher percentages in other studies conducted for deep-sea sediments (e.g., Woodall et al., 2014). The abundance of microfibers is consistent with the reported polymer types, as microfibers used in textiles are commonly made of polyester, polyamide, and acrylic (Henry et al., 2019). Other factors have also been linked with the abundance of microfibers in deep-sea sediments. Owing to their distinct shape, Kane and Clare (2019) suggested that microfibers can be transported by gravity currents to deeper sediments. Furthermore, as discussed in this paper, microfibers possess a larger exterior surface to volume ratio, which would lead to fast alteration in buoyancy if exposed to biofouling. The combination of brittleness and density of these polymers with the unique shape of microfibers leads to their intrusion into deep-sea sediments.

For offshore surface water, a compilation by Erni-Cassola et al. (2019) shows that more than 75% of polymers present are either PP or PE, while the demand for these 2 polymers combined is about 50%. These polymers are ductile and are not easily fragmented. As described in this study, in this compartment, MPs have a larger mean particle size. Due to their size, stemming from their slow fragmentation, these plastics remain afloat as

they are associated with larger Stokes numbers. Moreover, among the studies compiled here for surface water offshore, all have provided shape categories. Aside from Enders et al. (2015), all studies in this category have identified fragments as the dominant shape which was also reported by Woodall et al. (2014), among others. The combination of buoyancy and slow fragmentation rate leads to the presence of PP and PE particles in the surface, which is also related to a higher concentration of larger fragments in this compartment.

In nearshore surface water, however, authors did not find a consistently dominant shape in various studies. While Qu et al. (2018) reported fibers as the dominant shape, other studies such as Song et al. (2014) have reported fragments to be dominant. Furthermore, polymer analysis, conducted by Erni-Cassola et al. (2019) in the intertidal region, has shown the presence of multiple polymer types. This is likely due to the closer proximity of nearshore water to both marine and terrestrial plastic sources. Due to source variability in different geographical regions, plastic shapes and polymers found in studies conducted in the nearshore water are diverse.

As noted by Schwarz et al. (2019), the abundance of PVC in all freshwater and marine compartments is very low, while its production comprises about 10% of plastic demand. PVC is mainly used in building and construction (Plastics Europe, 2020) and, due to its extended life-cycle and better end-of-life waste management, provides a smaller contribution to freshwater and marine plastic pollution. Similarly, PUR is highly used in automotive and building and construction sectors, hence they also have not been reported in high concentrations in aquatic systems. PS is the polymer with the smallest elongation listed in **Table 2**. This polymer has been reported in various environmental compartments in both freshwater and marine surface and sediment samples (Erni-Cassola et al., 2019; Schwarz et al., 2019). This is due to the small marginal density of this polymer, $(\rho_p - \rho_w)$, combined with fast fragmentation. Once broken down into fine MPs, PS particles behave similarly to a passive scalar and disperse easily with the flow.

DISCUSSION AND RECOMMENDATION FOR FUTURE WORK

Aside from hydrodynamic and environmental factors, MPS' mobility is affected by their properties. These properties include polymer density, particle shape, and size. Motion of a MP particle, even in a quiescent fluid, is affected by all three properties: density dominates the buoyancy of the particle, shape affects the drag force, and size affects the magnitude of buoyant and gravitational forces as well as the magnitude of the drag force. Significant emphasis has been put on plastic density in the literature, as it is undeniably a critical factor in the distribution of plastics. Furthermore, to understand the mobility of MPs in terms of natural sediment particles, efforts have been made to define MPs by shape categories and, accordingly, define shape factors (Camenen, 2007; Kowalski et al., 2016). MP shape is also strongly linked to biofouling. The analogy with sediment particles infers that MP size is another important driver in MP distribution and mobility. Our assessment of several hydrodynamic factors,

namely relaxation time, settling and rise velocity, and Shields parameter indicates that MP particle size is directly tied to these parameters. Smaller-sized MPs exhibit lower relaxation time, lower settling velocity, faster onset of sinking if exposed to biofouling, and a lower Shields number.

These parameters affect the mobility of MP particles and their transport to regions distant from their source of emission. Our analysis of 15 studies that have provided size distribution for different regions of marine systems, also confirms this correlation. Nearshore surface water samples that are often closer to the emission source have exhibited a smaller D_{50}, while offshore surface water samples have shown a larger D_{50}, where aged plastics have undergone weathering and smaller MPs should be more abundant. This trend has been previously attributed to biofouling and faster onset of sinking for small MPs (Kooi et al., 2017). Our analysis suggests that other factors may contribute to the absence of small-sized MPs from the surface in offshore areas. Entrainment and in-depth mixing lead to the entrainment and long-distance transport of fine MPs. Similarly, small MPs can be entrained and advected with thermohaline circulation resulting in their deposit in remote Arctic areas. Furthermore, polymer fragmentation rates affect plastic size and, ultimately, its transport. Brittle polymers are fragmented into smaller MPs and are more abundant in far and remote areas. Along with microfibers' unique shape, this supports the presence of fibers in deep-sea sediments. On the other hand, polymers with slow fragmentation rates are found in larger fragment shapes in the offshore water surface. The studies that were presented in **Table 2** and analyzed in **Figures 4**, **5** were selected based on size distribution availability. However, these studies did not employ a standardized sampling, separation, and identification method or protocol. For in-depth and meaningful comparison and monitoring, it is critical to define and implement a standard method for all three steps to estimate the abundance, distribution, and composition of MPs. The size distribution range and bin sizes reported, therefore, were different since authors used different approaches. This has limited our analysis of existing literature and adds uncertainty to the analysis. Hence, we have limited our discussion and examination of these studies to qualitative analysis and have not provided aggregated size ranges herein.

This study highlights the importance of MP size, along with polymer composition and shape, in their mobility. Given the lack of data in size distribution, future quantitative studies should carefully examine the size distribution and limitations imposed by sampling and analysis. In using the analogy with natural sediments in terms of MP size, further research is required to investigate the linkage between MP shape, size, and density. Unlike mineral sediments, MPs are versatile in terms of their density and shape. As outlined in this study, marginal density, shape, and size appear in most hydrodynamic parameters, therefore, the definition of size categories for MPs should include consideration for other MP properties.

AUTHOR CONTRIBUTIONS

AS contributed to the core concept, conducted literature review, prepared the figures and tables, and contributed to the manuscript. ZL conducted literature review and contributed to the manuscript. PP conducted literature review, prepared tables, and contributed to the manuscript. SK contributed to ideation and core concept, supervised students, and wrote the manuscript. All authors contributed to the article and approved the submitted version.

FUNDING

REFERENCES

Adams, J. K., Dean, B. Y., Athey, S. N., Jantunen, L. M., Bernstein, S., Stern, G., et al. (2021). Anthropogenic particles (including microfibers and microplastics) in marine sediments of the Canadian Arctic. *Sci. Total Environ.* 784:147155. doi: 10.1016/j.scitotenv.2021.147155

Anderson, J. C., Park, B. J., and Palace, V. P. (2016). Microplastics in aquatic environments: implications for Canadian ecosystems. *Environ. Pollut.* 218, 269–280. doi: 10.1016/j.envpol.2016.06.074

Andrady, A. L. (2011). Microplastics in the marine environment. *Mar. Pollut. Bull.* 62, 1596–1605.

Artham, T., Sudhakar, M., Venkatesan, R., Nair, C. M., Murty, K. V. G. K., and Doble, M. (2009). Biofouling and stability of synthetic polymers in sea water. *Int. Biodeterior. Biodegradation* 63, 884–890.

Baldwin, A. K., Corsi, S. R., and Mason, S. A. (2016). Plastic debris in 29 Great Lakes tributaries: relations to watershed attributes and hydrology. *Environ. Sci. Technol.* 50, 10377–10385. doi: 10.1021/acs.est.6b02917

Ballent, A., Corcoran, P. L., Madden, O., Helm, P. A., and Longstaffe, F. J. (2016). Sources and sinks of microplastics in Canadian Lake Ontario nearshore, tributary and beach sediments. *Mar. Pollut. Bull.* 110, 383–395. doi: 10.1016/j. marpolbul.2016.06.037

Ballent, A., Purser, A., de Jesus Mendes, P., Pando, S., and Thomsen, L. (2012). Physical transport properties of marine microplastic pollution. *Biogeosci. Discuss.* 9, 18755–18798.

Barrett, J., Chase, Z., Zhang, J., Holl, M. M. B., Willis, K., Williams, A., et al. (2020). Microplastic pollution in deep-sea sediments from the great Australian bight. *Front. Mar. Sci.* 7:576170. doi: 10.3389/fmars.2020.57 6170

Bergmann, M., Wirzberger, V., Krumpen, T., Lorenz, C., Primpke, S., Tekman, M. B., et al. (2017). High quantities of microplastic in Arctic deep-sea sediments from the HAUSGARTEN observatory. *Environ. Sci. Technol.* 51, 11000–11010. doi: 10.1021/acs.est.7b03331

Camenen, B. (2007). Simple and general formula for the settling velocity of particles. *J. Hydraulic Eng.* 133, 229–233. doi: 10.1061/(ASCE)0733-9429(2007) 133:2(229)

Chae, D. H., Kim, I. S., Kim, S. K., Song, Y. K., and Shim, W. J. (2015). Abundance and distribution characteristics of microplastics in surface seawaters of the Incheon/Kyeonggi coastal region. *Arch. Environ. Contam. Toxicol.* 69, 269–278. doi: 10.1007/s00244-015-0173-4

Chiba, S., Saito, H., Fletcher, R., Yogi, T., Kayo, M., Miyagi, S., et al. (2018). Human footprint in the abyss: 30 year records of deep-sea plastic debris. *Mar. Policy* 96, 204–212.

Chubarenko, I., Bagaev, A., Zobkov, M., and Esiukova, E. (2016). On some physical and dynamical properties of microplastic particles in marine environment. *Mar. Pollut. Bull.* 108, 105–112.

Chubarenko, I., Esiukova, E., Bagaev, A., Isachenko, I., Demchenko, N., Zobkov, M., et al. (2018). "Behavior of microplastics in coastal zones," in *Microplastic Contamination In Aquatic Environments*, ed. E. Y. Zeng (Amsterdam: Elsevier), 175–223.

Clark, J. R., Cole, M., Lindeque, P. K., Fileman, E., Blackford, J., Lewis, C., et al. (2016). Marine microplastic debris: a targeted plan for understanding and quantifying interactions with marine life. *Front. Ecol. Environ.* 14:317–324. doi: 10.1002/fee.1297

Clift, R., Grace, J. R., and Weber, M. E. (1978). "Nonspherical rigid particles at higher Reynolds numbers," in *Bubbles Drops and Particles*, eds R. Clift, J. R. Grace, M. E. Weber, and M. F. Weber (Cambridge, MA: Academic Press), 142–168.

Cole, M., Lindeque, P., Fileman, E., Halsband, C., Goodhead, R., Moger, J., et al. (2013). Microplastic ingestion by zooplankton. *Environ. Sci. Technol.* 47, 6646–6655.

Cordova, M. R., and Wahyudi, A. (2016). Microplastic in the deep-sea sediment of Southwestern Sumatran Waters. *Mar. Res. Indones.* 41, 27–35.

Courtene-Jones, W., Quinn, B., Ewins, C., Gary, S. F., and Narayanaswamy, B. E. (2020). Microplastic accumulation in deep-sea sediments from the Rockall Trough. *Mar. Pollut. Bull.* 154:111092. doi: 10.1016/j.marpolbul.2020.111092

Cózar, A., Echevarría, F., González-Gordillo, J. I, Irigoien, X., Úbeda, B., Hernández-León, S., et al. (2014). Plastic debris in the open ocean. *Proc. Natl. Acad. Sci. U.S.A.* 111, 10239–10244.

Cózar, A., Martí, E., Duarte, C. M., García-de-Lomas, J., Van Sebille, E., Ballatore, T. J., et al. (2017). The Arctic Ocean as a dead end for floating plastics in the North Atlantic branch of the Thermohaline Circulation. *Sci. Adv.* 3:e1600582. doi: 10.1126/sciadv.1600582

Cunningham, E. M., Ehlers, S. M., Dick, J. T., Sigwart, J. D., Linse, K., Dick, J. J., et al. (2020). High abundances of microplastic pollution in deep-sea sediments: evidence from Antarctica and the Southern Ocean. *Environ. Sci. Technol.* 54, 13661–13671. doi: 10.1021/acs.est.0c03441

Dalu, T., Banda, T., Mutshekwa, T., Munyai, L. F., and Cuthbert, R. N. (2021). Effects of urbanisation and a wastewater treatment plant on microplastic densities along a subtropical river system. *Environ. Sci. Pollut. Res.* 28, 36102–36111. doi: 10.1007/s11356-021-13185-1

Dey, S., Zeeshan Ali, S., and Padhi, E. (2019). Terminal fall velocity: the legacy of Stokes from the perspective of fluvial hydraulics. *Proc. R. Soc. A* 475:20190277. doi: 10.1098/rspa.2019.0277

Di, M., and Wang, J. (2018). Microplastics in surface waters and sediments of the Three Gorges Reservoir, China. *Sci. Total Environ.* 616, 1620–1627.

Efimova, I., Bagaeva, M., Bagaev, A., Kileso, A., and Chubarenko, I. P. (2018). Secondary microplastics generation in the sea swash zone with coarse bottom sediments: laboratory experiments. *Front. Mar. Sci.* 5:313. doi: 10.3389/fmars.2018.00313

Enders, K., Lenz, R., Stedmon, C. A., and Nielsen, T. G. (2015). Abundance, size and polymer composition of marine microplastics $\geq$ 10 μm in the Atlantic Ocean and their modelled vertical distribution. *Mar. Pollut. Bull.* 100, 70–81. doi: 10.1016/j.marpolbul.2015.09.027

Erni-Cassola, G., Zadjelovic, V., Gibson, M. I., and Christie-Oleza, J. A. (2019). Distribution of plastic polymer types in the marine environment; a meta-analysis. *J. Hazard. Mater.* 369, 691–698. doi: 10.1016/j.jhazmat.2019.02.067

Fazey, F. M., and Ryan, P. G. (2016). Biofouling on buoyant marine plastics: an experimental study into the effect of size on surface longevity. *Environ. Pollut.* 210, 354–360. doi: 10.1016/j.envpol.2016.01.026

Filella, M. (2015). Questions of size and numbers in environmental research on microplastics: methodological and conceptual aspects. *Environ. Chem.* 12, 527–538.

Finn, J. R., Li, M., and Apte, S. V. (2016). Particle based modelling and simulation of natural sand dynamics in the wave bottom boundary layer. *J. Fluid Mech.* 796, 340–385.

Fossi, M. C., Panti, C., Guerranti, C., Coppola, D., Giannetti, M., Marsili, L., et al. (2012). Are baleen whales exposed to the threat of microplastics? A case study of the Mediterranean fin whale (*Balaenoptera physalus*). *Mar. Pollut. Bull.* 64, 2374–2379. doi: 10.1016/j.marpolbul.2012.08.013

Good, G. H., Ireland, P. J., Bewley, G. P., Bodenschatz, E., Collins, L. R., and Warhaft, Z. (2014). Settling regimes of inertial particles in isotropic turbulence. *J. Fluid Mech.* 759:R3. doi: 10.1103/PhysRevLett.117.064501

Gorokhovski, M., and Zamansky, R. (2018). Modeling the effects of small turbulent scales on the drag force for particles below and above the Kolmogorov scale. *Phys. Rev. Fluids* 3:034602.

Harper, C. A., and Petrie, E. M. (2003). *Plastics Materials And Processes: A Concise Encyclopedia*. Hoboken, NJ: John Wiley & Sons.

Heitmuller, F. T., and Hudson, P. F. (2009). Downstream trends in sediment size and composition of channel-bed, bar, and bank deposits related to hydrologic and lithologic controls in the Llano River watershed, central Texas, USA. *Geomorphology* 112, 246–260.

Henry, B., Laitala, K., and Klepp, I. G. (2019). Microfibres from apparel and home textiles: prospects for including microplastics in environmental sustainability assessment. *Sci. Total Environ.* 652, 483–494. doi: 10.1016/j.scitotenv.2018.10.166

Hidalgo-Ruz, V., Gutow, L., Thompson, R. C., and Thiel, M. (2012). Microplastics in the marine environment: a review of the methods used for identification and quantification. *Environ. Sci. Technol.* 46, 3060–3075.

Huntington, A., Corcoran, P. L., Jantunen, L., Thaysen, C., Bernstein, S., Stern, G. A., et al. (2020). A first assessment of microplastics and other anthropogenic particles in Hudson Bay and the surrounding eastern Canadian Arctic waters of Nunavut. *Facets* 5, 432–454.

Inman, D. L., and Bagnold, R. A. (1963). "Beach and nearshore processes. Part II. Littoral processes," in *The Sea: Ideas and Observations*, ed. M. N. Hille (Cambridge, MA: Harvard University Press), 529–553.

Inman, D. L., and Masters, P. M. (1991). "Coastal sediment transport concepts and mechanisms," in *Coast of California Storm and Tidal Waves Study: State of the Coast Report*, (Los Angeles, CA: U.S. Army Corps of Engineers). Available online at: https://escholarship.org/uc/item/8tc9x82q

Kaiser, D., Kowalski, N., and Waniek, J. J. (2017). Effects of biofouling on the sinking behavior of microplastics. *Environ. Res. Lett.* 12:124003.

Kane, I. A., and Clare, M. A. (2019). Dispersion, accumulation, and the ultimate fate of microplastics in deep-marine environments: a review and future directions. *Front. Earth Sci.* 7:80.

Kane, I. A., Clare, M. A., Miramontes, E., Wogelius, R., Rothwell, J. J., Garreau, P., et al. (2020). Seafloor microplastic hotspots controlled by deep-sea circulation. *Science* 368, 1140–1145. doi: 10.1126/science.aba5899

Karimpour, S., and Chu, V. H. (2019). The role of waves on mixing in shallow waters. *Can. J. Civil Eng.* 46, 134–147.

Karimpour, S., Wang, T., and Chu, V. H. (2021b). The exchanges between the mainstream in an open channel and a recirculating flow on its side at large Froude numbers. *J. Fluid Mech.* 920:A8.

Karimpour, S., Brar, S. K., and Shirkhani, H. (2021a). *The Fate And Transport Of Microplastics In Aquatic Ecosystems: Synthesis And Directions For Future Research*. Ottawa, ONT: Social Sciences and Humanities Research Council (SSHRC) of Canada.

Khatmullina, L., and Isachenko, I. (2017). Settling velocity of microplastic particles of regular shapes. *Mar. Pollut. Bull.* 114, 871–880. doi: 10.1016/j.marpolbul.2016.11.024

Kooi, M., Nes, E. H. V., Scheffer, M., and Koelmans, A. A. (2017). Ups and downs in the ocean: effects of biofouling on vertical transport of microplastics. *Environ. Sci. Technol.* 51, 7963–7971. doi: 10.1021/acs.est.6b04702

Kowalski, N., Reichardt, A. M., and Waniek, J. J. (2016). Sinking rates of microplastics and potential implications of their alteration by physical, biological, and chemical factors. *Mar. Pollut. Bull.* 109, 310–319. doi: 10.1016/j.marpolbul.2016.05.064

Lagarde, F., Olivier, O., Zanella, M., Daniel, P., Hiard, S., and Caruso, A. (2016). Microplastic interactions with freshwater microalgae: hetero-aggregation and changes in plastic density appear strongly dependent on polymer type. *Environ. Pollut.* 215, 331–339. doi: 10.1016/j.envpol.2016.05.006

Lehtiniemi, M., Hartikainen, S., Näkki, P., Engström-Öst, J., Koistinen, A., and Setälä, O. (2018). Size matters more than shape: ingestion of primary and secondary microplastics by small predators. *Food Webs* 17:e00097.

Long, M., Moriceau, B., Gallinari, M., Lambert, C., Huvet, A., Raffray, J., et al. (2015). Interactions between microplastics and phytoplankton aggregates: impact on their respective fates. *Mar. Chem.* 175, 39–46.

Lusher, A. (2015). "Microplastics in the marine environment: distribution, interactions and effects," in *Marine Anthropogenic Litter*, eds M. Bergmann, L. Gutow, and M. Klages (Cham: Springer), 245–307.

Miller, M. C., McCave, I. N., and Komar, P. (1977). Threshold of sediment motion under unidirectional currents. *Sedimentology* 24, 507–527.

Moore, C. J., Moore, S. L., Leecaster, M. K., and Weisberg, S. B. (2001). A comparison of plastic and plankton in the North Pacific central gyre. *Mar. Pollut. Bull.* 42, 1297–1300. doi: 10.1016/s0025-326x(01)00114-x

Morét-Ferguson, S., Law, K. L., Proskurowski, G., Murphy, E. K., Peacock, E. E., and Reddy, C. M. (2010). The size, mass, and composition of plastic debris in the western North Atlantic Ocean. *Mar. Pollut. Bull.* 60, 1873–1878. doi: 10.1016/j.marpolbul.2010.07.020

Mu, J., Qu, L., Jin, F., Zhang, S., Fang, C., Ma, X., et al. (2019). Abundance and distribution of microplastics in the surface sediments from the northern Bering and Chukchi Seas. *Environmental Pollution* 245, 122–130. doi: 10.1016/j.envpol.2018.10.097

Murphy, F., Ewins, C., Carbonnier, F., and Quinn, B. (2016). Wastewater treatment works (WwTW) as a source of microplastics in the aquatic environment. *Environ. Sci. Technol.* 50, 5800–5808.

Naidoo, T., Glassom, D., and Smit, A. J. (2015). Plastic pollution in five urban estuaries of KwaZulu-Natal, South Africa. *Mar. Pollut. Bull.* 101, 473–480. doi: 10.1016/j.marpolbul.2015.09.044

Napper, I. E., Davies, B. F., Clifford, H., Elvin, S., Koldewey, H. J., Mayewski, P. A., et al. (2020). Reaching new heights in plastic pollution—preliminary findings of microplastics on Mount Everest. *One Earth* 3, 621–630.

Plastics Europe (2020). *Plastics – The Facts 2020: An Analysis Of European Plastics Production, Demand And Waste Data*. Brussels: Plastic Europe.

Qu, X., Su, L., Li, H., Liang, M., and Shi, H. (2018). Assessing the relationship between the abundance and properties of microplastics in water and in mussels. *Sci. Total Environ.* 621, 679–686.

Radko, T. (2019). Thermohaline-shear instability. *Geophys. Res. Lett.* 46, 822–832.

Rebesco, M., Hernández-Molina, F. J., Van Rooij, D., and Wåhlin, A. (2014). Contourites and associated sediments controlled by deep-water circulation processes: state-of-the-art and future considerations. *Mar. Geol.* 352, 111–154.

Reisser, J., Slat, B., Noble, K., Du Plessis, K., Epp, M., Proietti, M., et al. (2015). The vertical distribution of buoyant plastics at sea: an observational study in the North Atlantic Gyre. *Biogeosciences* 12, 1249–1256.

Rochman, C. M., Hoh, E., Kurobe, T., and Teh, S. J. (2013). Ingested plastic transfers hazardous chemicals to fish and induces hepatic stress. *Sci. Rep.* 3, 1–7. doi: 10.1038/srep03263

Rummel, C. D., Jahnke, A., Gorokhova, E., Kühnel, D., and Schmitt-Jansen, M. (2017). Impacts of biofilm formation on the fate and potential effects of microplastic in the aquatic environment. *Environ. Sci. Technol. Lett.* 4, 258–267.

Ryan, P. G. (2015). Does size and buoyancy affect the long-distance transport of floating debris? *Environ. Res. Lett.* 10:084019.

Sagawa, N., Kawaai, K., and Hinata, H. (2018). Abundance and size of microplastics in a coastal sea: comparison among bottom sediment, beach sediment, and surface water. *Mar. Pollut. Bull.* 133, 532–542. doi: 10.1016/j.marpolbul.2018.05.036

Schwarz, A. E., Ligthart, T. N., Boukris, E., and Van Harmelen, T. (2019). Sources, transport, and accumulation of different types of plastic litter in aquatic environments: a review study. *Mar. Pollut. Bull.* 143, 92–100. doi: 10.1016/j.marpolbul.2019.04.029

Shields, A. (1936). *Application Of Similarity Principles And Turbulence Research To Bed-Load Movement*. Pasadena, CA: California Institute of Technology.

Song, Y. K., Hong, S. H., Jang, M., Kang, J. H., Kwon, O. Y., Han, G. M., et al. (2014). Large accumulation of micro-sized synthetic polymer particles in the sea surface microlayer. *Environ. Sci. Technol.* 48, 9014–9021. doi: 10.1021/es501757s

Suaria, G., Avio, C. G., Mineo, A., Lattin, G. L., Magaldi, M. G., Belmonte, G., et al. (2016). The mediterranean plastic soup: synthetic polymers in mediterranean surface waters. *Sci. Rep.* 6, 1–10. doi: 10.1038/srep37551

Tanaka, K., and Takada, H. (2016). Microplastic fragments and microbeads in digestive tracts of planktivorous fish from urban coastal waters. *Sci. Rep.* 6, 1–8. doi: 10.1038/srep34351

Tekman, M. B., Wekerle, C., Lorenz, C., Primpke, S., Hasemann, C., Gerdts, G., et al. (2020). Tying up loose ends of microplastic pollution in the Arctic: distribution from the sea surface through the water column to deep-sea sediments at the Hausgarten observatory. *Environ. Sci. Technol.* 54, 4079–4090. doi: 10.1021/acs.est.9b06981

Teuten, E. L., Rowland, S. J., Galloway, T. S., and Thompson, R. C. (2007). Potential for plastics to transport hydrophobic contaminants. *Environ. Sci. Technol.* 41, 7759–7764.

Thompson, R. C., Olsen, Y., Mitchell, R. P., Davis, A., Rowland, S. J., John, A. W., et al. (2004). Lost at sea: where is all the plastic? *Science (Washington)* 304, 838.

Van Cauwenberghe, L., Vanreusel, A., Mees, J., and Janssen, C. R. (2013). Microplastic pollution in deep-sea sediments. *Environ. Pollut.* 182, 495–499.

Van Sebille, E., Aliani, S., Law, K. L., Maximenko, N., Alsina, J. M., Bagaev, A., et al. (2020). The physical oceanography of the transport of floating marine debris. *Environ. Res. Lett.* 15:023003.

Waldschläger, K., and Schüttrumpf, H. (2019). Effects of particle properties on the settling and rise velocities of microplastics in freshwater under laboratory conditions. *Environ. Sci. Technol.* 53, 1958–1966. doi: 10.1021/acs.est.8b06794

Waldschläger, K., Born, M., Cowger, W., Gray, A., and Schüttrumpf, H. (2020). Settling and rising velocities of environmentally weathered micro-and macroplastic particles. *Environ. Res.* 191:110192. doi: 10.1016/j.envres.2020.110192

Wang, L. P., and Maxey, M. R. (1993). Settling velocity and concentration distribution of heavy particles in homogeneous isotropic turbulence. *J. Fluid Mech.* 256, 27–68.

Wang, Y., Lam, K. M., and Lu, Y. (2018). Settling velocity of fine heavy particles in turbulent open channel flow. *Phys. Fluids* 30:095106.

Woodall, L. C., Sanchez-Vidal, A., Canals, M., Paterson, G. L., Coppock, R., Sleight, V., et al. (2014). The deep sea is a major sink for microplastic debris. *R. Soc. Open Sci.* 1:140317.

Xiao, F., Li, X., Lam, K., and Wang, D. (2012). Investigation of the hydrodynamic behavior of diatom aggregates using particle image velocimetry. *J. Environ. Sci.* 24, 1157–1164. doi: 10.1016/s1001-0742(11)60960-1

Yang, H., and Shi, C. (2019). Sediment grain-size characteristics and its sources of ten wind-water coupled erosion tributaries (the Ten Kongduis) in the Upper Yellow River. *Water* 11:115.

Ye, S., and Andrady, A. L. (1991). Fouling of floating plastic debris under Biscayne Bay exposure conditions. *Mar. Pollut. Bull.* 22, 608–613.

Zhang, D., Liu, X., Huang, W., Li, J., Wang, C., Zhang, D., et al. (2020). Microplastic pollution in deep-sea sediments and organisms of the Western Pacific Ocean. *Environ. Pollut.* 259:113948. doi: 10.1016/j.envpol.2020.113948

Zhang, H. (2017). Transport of microplastics in coastal seas. *Estuar. Coast. Shelf Sci.* 199, 74–86.